Structural Studies of Wild-Type and Mutant Reaction Centers from an Antenna-Deficient Strain of *Rhodobacter sphaeroides*: Monitoring the Optical Properties of the Complex from Bacterial Cell to Crystal†

Katherine E. McAuley-Hecht,§ Paul K. Fyfe,§ Justin P. Ridge,‖ Steve M. Prince,⊥ C. Neil Hunter,‖ Neil W. Isaacs,⊥ Richard J. Cogdell,§ and Michael R. Jones*,‖

Division of Biochemistry and Molecular Biology and Department of Chemistry, University of Glasgow, Glasgow G12 8QQ, United Kingdom, and Krebs Institute for Biomolecular Research and Robert Hill Institute for Photosynthesis, Department of Molecular Biology and Biotechnology, University of Sheffield, Western Bank, Sheffield S10 2UH, United Kingdom

Received July 14, 1997; Revised Manuscript Received January 15, 1998

ABSTRACT: Reaction centers have been crystallized from the antenna-deficient RCO2 strain of *Rhodobacter sphaeroides*, and a structural model has been constructed at 2.6 Å resolution. The antenna-deficient strain allows assessment of the structural integrity of the reaction center at each stage in the purification−crystallization procedure. Spectroscopic evidence indicates that the properties of the reaction center bacteriopheophytins and the primary donor bacteriochlorophylls are modified somewhat on removal of the protein complex from the membrane and that these changes are carried through to the crystal form of the reaction center. The structure of a FM197R/YM177F mutant reaction center has also been determined to 2.55 Å resolution. The mutant complex shows an unexpected change in structure, with a significant reorientation of the new arginine, the incorporation of a new water molecule into the structure, and rotation of the 2-acetyl carbonyl group of one of the primary donor bacteriochlorophylls to a more out-of-plane geometry. Changes in the optical spectrum of the FM197R/YM177F reaction center are discussed with respect to the altered structure of the complex.

The photosynthetic reaction center (RC)[1] is an integral membrane protein that is responsible for the transduction of light energy into chemical energy in photosynthetic bacteria, algae, and higher plants. The best understood RCs are those from purple non-sulfur photosynthetic bacteria such as *Rhodopseudomonas* (*Rps.*) *viridis*, *Rhodobacter* (*Rb*) *sphaeroides*, and *Rhodobacter capsulatus*. The catalyst for much of the detailed research carried out on the RC over the last 10 years was undoubtedly the elucidation of the high-resolution X-ray structure of the *Rps. viridis* RC (*1, 2*), followed shortly afterward by the structure of the RC from *Rb. sphaeroides* (*3*−*7*). These X-ray structures confirmed many predictions concerning the structure and mechanism of the RC that had arisen from spectroscopic studies of the complex (reviewed in refs *8* and *9*).

In *Rb. sphaeroides*, the RC consists of three protein subunits: H, L, and M. The L and M subunits each have five transmembrane helices and are related by an axis of approximate 2-fold symmetry (*3*−*7*). The H subunit has a single transmembrane helix and caps the cytoplasmic faces of the L and M subunits. The bacteriochlorin and quinone cofactors are encased by the L and M subunits and are arranged in two branches that span the membrane. Only one of these branches is active in transmembrane electron transfer. Spectroscopic studies have revealed the route of electron transfer through the complex (*8*, *9*). The primary donor of electrons (P) is a pair of excitonically coupled bacteriochlorophyll (Bchl) molecules that lie close to the periplasmic face of the protein. Electrons are passed from P to one of a pair of symmetrically arranged bacteriopheophytin (Bphe) molecules, located approximately halfway across the membrane. The electron transfer probably proceeds via a monomeric Bchl that lies between P and the acceptor Bphe (*10*). The electron is passed on from the Bphe to a molecule of ubiquinone that lies close to the cytoplasmic side of the membrane, thus generating a transmembrane electrical potential. Knowledge of the fine detail of the structure of the RC has allowed examination of the mechanism of light-driven electron transfer through protein engineering. In recent years, site-directed mutagenesis and random mutagenesis have generated RCs with altered properties, providing new experimental material (see refs *11* and *12* for reviews).

† This work was supported by the Biotechnology and Biological Sciences Research Council of the U.K. and the Human Frontier Science Programme. M.R.J. is a BBSRC Advanced Research Fellow, and P.K.F. and J.P.R. are BBSRC Postgraduate Students. P.K.F. thanks the European Science Foundation for the opportunity to spend time in the laboratory of Günter Fritzsch in Frankfurt and to acknowledge the assistance received during the visit.

‡ The coordinates have been deposited with the Brookhaven Protein Data Bank under identification code 1MPS.

* Correspondence should be addressed to this author at Department of Molecular Biology and Biotechnology, University of Sheffield, Western Bank, Sheffield S10 2UH, United Kingdom. Fax: 44-114-2728697. E-mail: m.jones@sheffield.ac.uk.

§ Division of Biochemistry and Molecular Biology, University of Glasgow.

‖ University of Sheffield.

⊥ Department of Chemistry, University of Glasgow.

[1] Abbreviations: Bchl, bacteriochlorophyll; Bphe, bacteriopheophytin; LDAO, lauryldimethylamine oxide; P, primary donor; RC, reaction center; Ubi, ubiquinone; Spo, spheroidenone; WT, wild type.

S0006-2960(97)01717-0 CCC: $15.00
Published on Web 03/19/1998

When the properties of mutated RCs are being considered, high-resolution structural information on the altered complex is extremely valuable, providing a sound basis for the interpretation of spectroscopic data in terms of changes in cofactor−cofactor and cofactor−protein interactions. Despite this, relatively few mutant structures have been described (*13*, *14*). Part of the reason for this is the difficulty in obtaining crystals of integral membrane proteins that diffract to sufficient resolution. An illustration of this problem is the fact that to date no structure has been forthcoming for the *Rb. capsulatus* RC, despite it showing a similarity to the *Rb. sphaeroides* RC that is sufficiently close to have allowed a structural model to be made (*15*). In addition, high-resolution structures are still needed for the higher plant RCs despite considerable research effort in this area. Most progress has been made in the photosystem I reaction center from *Synechococcus*, for which a structure at 4 Å has recently been reported (*16*).

In 1992, a genetic system was described that allows the construction of a strain of *Rb. sphaeroides* lacking the antenna pigment−protein complexes (*17*). The principal advantage of this strain is that it allows study of the RC while it is still in the bacterial membrane, and a number of reports have since sought to compare the properties of the membrane-bound form of the *Rb. sphaeroides* RC with the detergent-solubilized form (*18*−*20*). The strain also provides an alternative means of studying the properties of mutant RC complexes (*21*, *22*), which have the potential to show altered tolerances to detergent. In addition, access to the optical properties of the RC in both cells and membranes means that the integrity of the RC can be assessed at each stage in RC purification, including immediately before removal of the complex from the membrane. Although this feature is not so important for the wild-type (WT) *Rb. sphaeroides* RC, which is relatively robust, it allows monitoring of the state of mutant complexes, which may be far more sensitive to the biochemical treatments involved in their purification and crystallization.

In this report, we describe the process by which WT or mutant *Rb. sphaeroides* RCs expressed in a strain with an antenna-deficient phenotype can be removed from the membrane, purified, and crystallized. We illustrate how the spectroscopic properties of the RC can be monitored, up to and including the crystal form of the complex, and can be compared to the original, membrane-bound complex. The crystals obtained are of the trigonal form described by Michel and co-workers (*23*−*25*) and diffract to around 2.4 Å resolution. We compare the details of the X-ray structure obtained for the WT complex extracted from the RC-only source with previously reported structures. We also report the structure of a RC carrying two site-directed mutations. One of these, FM197R, is situated in the vicinity of the P Bchls, while the second, YM177F, is located in the binding pocket of the RC carotenoid. Changes in the optical spectrum of the mutant RC are discussed in the light of observed changes in the geometry of the P Bchls and other possible changes in protein structure.

MATERIALS AND METHODS

Mutagenesis. The mutations Phe M197 to Arg (FM197R) and Tyr M177 to Phe (YM177F) were introduced to the *pufM* gene in two sequential steps using mismatch oligonucleotides. The template for mutagenesis was plasmid pALTSB-1, which consisted of a 998 bp *Sal*I−*Bam*HI restriction fragment encompassing the 3′ end of the *pufL* gene and the whole of the *pufM* gene cloned into the plasmid pALTER-1 (Promega). The resulting changes in the sequence of the *pufM* gene were confined to the target M197 and M177 codons (TTC to CGC and TAC to TTC) and were confirmed by DNA sequencing. The mutated *Sal*I−*Bam*HI restriction fragment was then transferred to plasmid pRKEH10D for expression in the double-deletion/insertion mutant strain DD13 as described in detail in refs *17*, *18*, and *26*. The resulting strain, named FM197R/YM177F, lacked both the LH1 and LH2 antenna complexes and contained the mutant RC as the sole pigment−protein complex.

Media, Strains, Growth Conditions, and Preparation of Membranes. WT RCs were purified from the antenna-deficient control strain RCO2 (*27*) and from the FM197R/YM177F mutant strain described above. Both strains produce the WT carotenoids spheroidene and spheroidenone. The strains were grown under semiaerobic, dark conditions at 34 °C in M22+ medium supplemented with neomycin, streptomycin, and tetracycline, as described in ref *26*. Cultures were scaled up through 10 mL, 70 mL, and 1 L stages in an orbital incubator operating at 160 rpm. The 1 L culture was used to inoculate a flask containing 20 L of stirred M22+ medium which was aerated through a compressed air line with on-line filter sterilization (Millex-FG, 0.2 μm filters). Intracytoplasmic membranes were isolated by breakage of harvested cells in a French Pressure Cell, as described in ref *26*, followed by ultracentrifugation at ∼250000*g* for 1.5 h. Intracytoplasmic membranes were resuspended to a concentration of approximately 10 absorbance units cm^{-1} at 800 nm in 20 mM Tris/HCl (pH 8.0).

Purification of RCs. RCs were isolated from resuspended intracytoplasmic membranes by a method based on that described in ref *28*. Solid NaCl was added to the membranes to a final concentration of 100 mM, and the suspension was stirred in the dark at room temperature. Lauryldimethylamine oxide (LDAO) (Fluka) was added to a final concentration of 0.3%, and the incubation was continued for 1.5 h. The suspension was then centrifuged at ∼250000*g* for 1.5 h, and the supernatant containing solubilized RCs was decanted. The membrane pellet was resuspended in 20 mM Tris/HCl (pH 8.0), and the NaCl/LDAO extraction was repeated either once or twice to ensure a maximal yield of RCs. Purification of the RCs was achieved by two passes of the solubilized material through a DE52 (Whatman) anion exchange column, followed by further anion exchange separation on a Sepharose Q column (Pharmacia). Chromatographic separation was performed with a stepped gradient of increasing NaCl concentrations in Tris/HCl (pH 8.0)/0.1% LDAO buffer. Elution of bound RCs from these ion exchange columns was achieved by washing the column with buffer containing 20 mM Tris/HCl (pH 8.0)/300 mM NaCl/0.1% LDAO. The RCs were further purified by gel filtration using a Superdex 200 preparative grade column (Pharmacia). Pooled RCs from the gel filtration column typically had an absorbance ratio A_{280}/A_{800} of 1.3. This ratio was used as a guide to the purity of the RC preparation, as described in ref *29*. The lower the ratio of A_{280}/A_{800}, the

higher the purity; samples with a ratio of <1.4 were found to be suitable for crystallization.

Purified RCs were concentrated by ultrafiltration, first in a stirred cell (Amicon) under nitrogen gas, and finally in Centricon concentrators (Amicon). After this initial concentration, the RCs were washed with the buffer required for crystallization [10 mM Tris/HCl (pH 8.0)/0.09% LDAO] and reconcentrated using Centricon concentrators. This washing was repeated at least five times to ensure good buffer exchange, and the RCs were brought to a final concentration of 60 absorbance units cm^{-1} at 800 nm, again in 10 mM Tris/HCl (pH 8.0)/0.09% LDAO.

Crystallography. The method used for growing trigonal crystals of the *Rb. sphaeroides* RC was based on that described in ref *23*. RC crystals were grown by vapor diffusion from sitting drops at 16 °C. A potassium phosphate solution (pH 7.5), 1,4-dioxane, and solid heptane-1,2,3-triol were added to the protein solution to give final concentrations of 0.75 M, 2% (v/v), and 3.5% (w/v), respectively. The droplets were equilibrated against a reservoir solution of 1.6 M potassium phosphate. Trigonal crystals appeared within 1−4 weeks and grew as prisms of variable size, ranging from 0.3 to 1 mm in the longest dimension. The crystals belonged to the space group $P3_121$ and had the following unit cell dimensions: $a = b = 142.4$ Å, $c = 188.6$ Å, $\alpha = \beta = 90°$, and $\gamma = 120°$ for the WT RC; $a = b = 141.9$ Å, $c = 187.9$ Å, $\alpha = \beta = 90°$, $\gamma = 120°$ for the mutant RC. The unit cell dimensions were very similar to those determined previously for the trigonal crystal form of the WT RC [$a = b = 141.4$ Å and $c = 187.2$ Å (*23*)].

The X-ray diffraction data were collected at room temperature on a 30 cm MAR image plate on station 9.6 of the Daresbury synchrotron facility. The crystal of the WT RC initially diffracted to 2.4 Å, though the resolution decreased during the data collection as a result of radiation damage. The crystal was translated twice to minimize this problem. Radiation damage led to a gradual loss of the high-resolution terms over time, so the effective isotropic resolution of the data set was limited to the resolution at which 50% of reflections in the outer shell had an I of $>2\sigma I$. The data were processed using the Denzo and Scalepack packages (*30*) to give an overall R_{merge} of 7.0% for data that was 94.9% complete to 2.6 Å, with 64 071 unique reflections for the WT RC. The data set acquired for the FM197R/YM177F mutant RC had an effective isotropic resolution of 2.55 Å. In this case, the overall R_{merge} was 12.9% for data that was 76.5% complete to 2.55 Å, with 54 163 unique reflections.

The structure of the WT RC was phased by molecular replacement using AMoRe (*31*), with the coordinates of the RC from *Rb. sphaeroides* strain ATCC 17023 (*24*, *25*) as the starting model, minus the detergent and water molecules. The rotational and translational searches, performed over the resolution range of 11−4 Å, yielded one clear solution. The correlation coefficient and *R*-factor for this solution were 85 and 24%, respectively. The model obtained from the molecular replacement was used as the starting point for the refinement of the mutant RC complex. After molecular replacement, the rotation matrix and translational values were (1.000, −0.0013, −0.0013, 0.0013, 1.000, −0.0025, 0.0013, 0.0025, 1.000), 0.112, −0.711, and −0.578.

Rigid-body refinement was performed using X-PLOR 3.1 (*32*), yielding *R*-factors of 34% for the WT RC and 33% for the mutant complex using the full resolution range. The mutated residues were omitted at this stage and rebuilt into omit density following simulated annealing refinement. Refinement continued with alternating rounds of positional or simulated annealing refinement in X-PLOR and manual rebuilding using the graphics program O (*33*). Water molecules were included only if they appeared with approximately spherical density in both the $2F_O - F_C$ and $F_O - F_C$ electron density maps and showed good hydrogen bonding geometry. The final refinement statistics are given in Table 1. The small difference between the values for the *R*-factor and R_{free} was almost certainly due to the fact that our models are isostructural with respect to that described by Ermler et al. (*24*, *25*) for the trigonal form of the RC. Although 5% of all reflections were omitted from our refinement, these have previously been included in the refinements of Ermler et al. Therefore, the R_{free} is not entirely free. The topology and parameter files used in X-PLOR for the cofactor groups were kindly supplied by U. Ermler, G. Fritzsch, and C. R. D. Lancaster. All computations used programs from the CCP4 suite (*34*) unless stated otherwise.

Table 1: Crystallographic Statistics for Data Collection and Refinement

	wild-type RC	FM197R/YM177F RC
collection statistics		
no. of unique reflections	64 071	54 163
completeness[a]	94.9% (98.4%)	76.5% (83.0%)
multiplicity	2.6 (2.5)	3.0 (2.3)
R_{merge}[a,b]	7.0% (42.0%)	12.9% (36.0%)
refinement statistics		
resolution range	11−2.6 Å	11−2.55 Å
no. of selected reflections where $F > \sigma F$	57 980	n/a
R-factor[c]	18.3%	19.4%
R_{free}[d]	20.4%	21.7%
average *B*-factor	50.1 Å^2	40.1 Å^2
geometry		
rmsd from ideality		
bonds	0.012 Å	0.008 Å
angles	1.68°	1.54°
residues in the Ramachandran plot[e]		
most favored areas	90.7%	90.9%
additional allowed areas	9.0%	8.7%
generously allowed areas	0.3%	0.4%
disallowed areas	0.0%	0.0%
coordinate error[f]	0.3 Å	0.35 Å
model		
no. of protein residues	823	823
no. of pigments	4 Bchl, 2 Bphe, 2 Ubi, 1 Spo, and 1 Fe	4 Bchl, 2 Bphe, 1 Ubi, 1 Spo, and 1 Fe
no. of waters	108	100
no. of detergents	4	3
no. of phosphates	0	1

[a] Figures within brackets refer to the statistics for the outer resolution shell (2.69−2.6 Å), and 2.64−2.55 Å for the mutant model. The completeness for the higher-resolution shell was higher than the overall completeness due to overloaded low-resolution reflections. [b] $R_{merge} = \sum_h\sum_i|\langle I(h)\rangle - I(h)_i|/\sum_h\sum_i I(h)_i$, where $I(h)$ is the intensity of reflection h, $\sum_h$ is the sum over all reflections, and $\sum_I$ is the sum over all i measurements of reflection h. [c] *R*-factor is defined by $\sum||F_O| - |F_C||/\sum|F_O|$. [d] R_{free} was calculated with 5% reflections, selected randomly (*53*), and these reflections were omitted from all refinement steps. [e] Ramachandran plot was produced by Procheck version 3.0 (*54*). [f] Coordinate error was estimated with a Luzzati plot (*55*).

Spectroscopy. Absorption spectra of bacterial cells, intact membranes, purified RCs, and RC crystals were obtained using a Guided Wave model 260 fiber optic spectrophotometer (Guided Wave Inc., El Dorado Hills, CA). Spectra of bacterial cells were obtained using aliquots taken from growing cultures in the late log phase. Membranes were diluted in 10 mM Tris/HCl (pH 8.0), while purified complexes were diluted in 20 mM Tris/HCl (pH 8.0)/0.1% LDAO. Because the Guided Wave spectrophotometer irradiates the sample with white light, resulting in bleaching of the P Q_y absorbance band, sodium ascorbate was added to a final concentration of 10 mM to ensure full reduction of the P Bchls [spectra recorded with a Beckman DU640 spectrophotometer showed that, in untreated crystals, the P Q_y band was not bleached when interrogated with weak monochromatic light (data not shown); the bleaching observed with the Guided Wave spectrophotometer was therefore due to the white light used and was not a consequence of the crystallization conditions]. Spectra of crystals were recorded by positioning the fiber optic cables above and below the wells of the crystal plate. Crystals were soaked in 5 mM sodium ascorbate for 3 h prior to acquisition of ascorbate-reduced spectra. This treatment did not adversely affect the gross morphology of the crystals during the period of the experiment. Light-oxidized spectra were recorded by omitting sodium ascorbate.

RESULTS

Monitoring of the Spectrum of the WT RC from Bacterial Cell to Crystal. The use of the antenna-deficient RCO2 strain allowed the absorption spectrum of the WT RC to be monitored at each stage of the growth/solubilization/purification/crystallization process. Figure 1A shows a series of room-temperature absorption spectra that provide a good indication of the structural integrity of the WT RC during the process that leads to RC crystals. The RC spectrum in the near-infrared region shows three principal absorbance bands that arise from the RC bacteriochlorin pigments. The band at 758 nm is attributed to the Q_y transitions of the two RC Bphes; the band at 804 nm is attributed to the Q_y transitions of the two monomeric Bchls and the high-energy exciton component of the Q_y transition of the P Bchls, and the band at 868 nm is attributed to the low-energy exciton component of the Q_y transition of the P Bchls. For convenience, we will use the terms Bphe Q_y band, Bchl Q_y band, and P Q_y band for the 758, 804, and 868 nm bands, respectively. The effect of detergent solubilization, purification, and crystallization on the optical properties of the RC was monitored by referencing the absorption spectrum of intracytoplasmic membranes, as this was of better quality than the spectrum of intact bacterial cells which was strongly affected by light scatter. Experiments with a large number of cultures of WT and mutant RC-only strains have shown that the preparation of membranes from intact cells does not affect the spectrum of the RC in any significant way (M. R. Jones, unpublished data).

Extraction of the WT RC from the membrane and purification of the complex had a small effect on the near-infrared absorption spectrum, with a 4 nm red shift of the Bphe Q_y band and a 2 nm blue shift of the P Q_y band (compare spectra "membrane" and "purified" in Figure 1A). Crystallization of the WT RC complex had little further effect

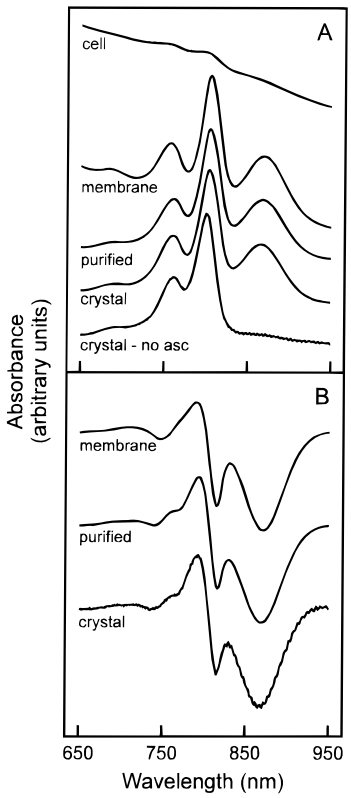

FIGURE 1: (A) Room-temperature absorption spectra for various forms of the WT RC from strain RCO2. Key: cell, bacterial cells; membrane, ascorbate-reduced intracytoplasmic membranes; purified, ascorbate-reduced purified RCs; crystal, ascorbate-reduced RC crystal; crystal-no asc, RC crystal (no sodium ascorbate). (B) Light-oxidized minus ascorbate-reduced difference spectra for various forms of the WT RC from strain RCO2. Same key as in panel A.

on the spectrum (spectrum "crystal" in Figure 1A). For crystals that had not been presoaked with sodium ascorbate, the P Q_y band was bleached due to photooxidation of P by the white measuring light of the spectrophotometer (see Materials and Methods). This bleaching was accompanied by an electrochromic blue shift of the absorbance band at 804 nm (to 800 nm) and a small sharpening of the Bphe Q_y band. The calculated light-oxidized minus ascorbate-reduced difference spectrum for the crystallized RC is shown in Figure 1B, where it is compared with difference spectra calculated for the membrane-bound and purified versions of the WT RC. Taken together, the spectroscopic data demonstrate that, while the overall structural and functional integrity of the WT RC was preserved on removal of the complex from the membrane, the change of environment was sensed by P and the Bphes. However, the optical properties of the complex did not seem to be perturbed any further by the processes of purification and crystallization.

Crystallography of the WT RC. The procedures used to obtain trigonal crystals of the WT RC from the antenna-deficient strain RCO2 are described in detail in Materials and Methods. RCs were purified by a standard procedure involving detergent solubilization followed by ion exchange chromatography and gel filtration. Trigonal crystals of varying sizes were obtained between 1 and 4 weeks, using a method based on that described in ref *23*. A crystal approximately 1.0 × 0.4 × 0.4 mm in size was used for the collection of X-ray data. A similar crystal was used to obtain the absorption spectra shown in Figure 1A.

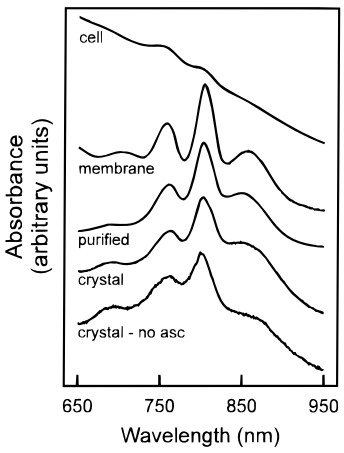

FIGURE 2: Room-temperature absorption spectra for various forms of a FM197R/YM177F mutant RC from an RC-only strain. Key as in the legend of Figure 1A.

After refinement, the structure of the RCO2 RC was found to be very similar to the 2.65 Å structure described in refs *24* and *25*. Superimposition of the α-carbons of the two RC structures gave a rms displacement of 0.35 Å. Structural conservation in the main body of the protein was very good, with a low degree of variance in the α-helical transmembrane regions. The residues showing the largest deviations were located on the outer surface of the protein and the C-terminal end of the H chain, and therefore did not represent inherent differences in structure and were unlikely to be of any functional significance. Those regions of the protein not resolved in the published 2.65 Å data (*24*, *25*) were also disordered in our map. These included the first 10 amino acids of the H chain, residues 251−260 of the C terminus of the H chain and residues 303−307 of the C terminus of the M chain.

Construction and Spectroscopy of the FM197R/YM177F Mutant RC. Residue Phe M197 is related by the axis of 2-fold symmetry that runs through the RC to residue His L168, which forms a H bond to the 2-acetyl carbonyl of the L side Bchl of P (P_L) (*35*). This H bond can be broken by mutagenesis of His L168 to Phe (*36*, *37*). Mutagenesis experiments have shown that substitution of Phe M197 by His or Tyr results in the formation of an analogous H bond to the 2-acetyl carbonyl group of P_M (*37*, *38*). The mutation Phe M197 to Arg described in this report was constructed as part of a survey of residues that are capable of forming a H bond interaction with the 2-acetyl carbonyl of P_M (M. R. Jones and J. P. Ridge, unpublished data). During this work, it was noted that the FM197R mutation (and a similar FM197K mutation) brought about a 15 nm blue shift of the P Q_y absorbance band (Figure 2). In contrast, there is no such blue shift in the room-temperature spectrum of a FM197Y or FM197H mutant either in solubilized RCs (*37*) or in RC-only membranes (M. R. Jones and J. P. Ridge, unpublished data). It should be noted that the FM197R mutant examined in this report carried a second mutation (YM177F) in the carotenoid binding pocket. Experiments conducted with an FM197R single mutant and a YM177F single mutant have shown that the spectrum of the RC bacteriochlorins in the Q_y region between 700 and 950 nm is not affected by the YM177F mutation (data not shown).

To investigate the structural origins of the blue shift of the P Q_y band in the FM197R and FM197R/YM177F RCs, crystals of the latter complex were prepared as described in Materials and Methods. The absorption spectra of various preparations of the FM197R/YM177F RC, including the crystal form, are shown in Figure 2. Once again, these data illustrate how the use of an antenna-deficient strain allows us to distinguish between structural changes that are associated directly with the mutation(s) that have been introduced and additional spectral shifts that occur following detergent solubilization or purification of the mutant RC. Comparison of the various forms of the FM197R/YM177F RC showed that the absorption maximum of the Bphe Q_y band underwent a small (3−4 nm) red shift on purification of the complex. This shift was similar to that seen in the purified and crystallized forms of the WT RC. The FM197R/YM177F RC also showed a 1−2 nm blue shift of the P Q_y band on removal of the complex from the membrane (Figure 2, spectra "membrane" and "purified").

Structure of the FM197R/YM177F RC. A data set with an isotropic resolution of 2.55 Å was collected at the Daresbury synchrotron facility using a crystal similar to that used to obtain the spectra shown in Figure 2. The structure of the FM197R/YM177F RC was then solved by molecular replacement to an effective isotropic resolution of 2.55 Å, as described in Materials and Methods. Comparison of the structure of the FM197R/YM177F RC with that of the WT RC showed good conservation of the overall structure throughout very nearly the entire volume of the protein. Within the resolution of the data, the replacement of Tyr by Phe at the M177 position caused no structural changes relative to the RCO2 RC other than the loss of the electron density associated with the Tyr OH group (Figure 3). In particular, the YM177F mutation did not appear to cause any change in the position of the carotenoid or any significant reduction in the occupancy of the binding pocket, as judged by the *B*-factor distribution in the carotenoid binding pocket of the protein and in the carotenoid itself. The average *B*-factor for the binding pocket was calculated for residues M115, M119, M122, M157, and M177 to be 41.7. These residues are located within the central region of the carotenoid binding pocket. The average *B*-factor for the carotenoid in the same region (atoms C10−C23) was 42.2. The methoxy end of the spheroidenone molecule is seen in the electron density maps, and this has allowed us to fit the cis bond at the 15−15′ position. However, the opposite end of the carotenoid molecule has four terminal atoms protruding from the protein, and the position of these atoms is not observed in the electron density maps. Conservation of the structure was good in the central region of the molecule which is fixed in the protein interior (Figure 3). We conclude from these data that the differences that were seen between the structure of the FM197R/YM177F RC and that of the WT complex in the vicinity of the P Bchls, described in detail in the next paragraph, could not be attributed to the YM177F mutation.

The FM197R mutation brought about a significant change in the structure of the protein in the immediate vicinity of the M197 residue, and also in the detailed structure of the P_L Bchl, as summarized in Figures 4 and 5. The Arg residue introduced in the FM197R/YM177F RC did not occupy the volume of the Phe residue that is present in the WT complex (Figures 4A and 5A) but rather pointed toward the periplasmic surface of the protein (Figures 4B and 5B). Rather

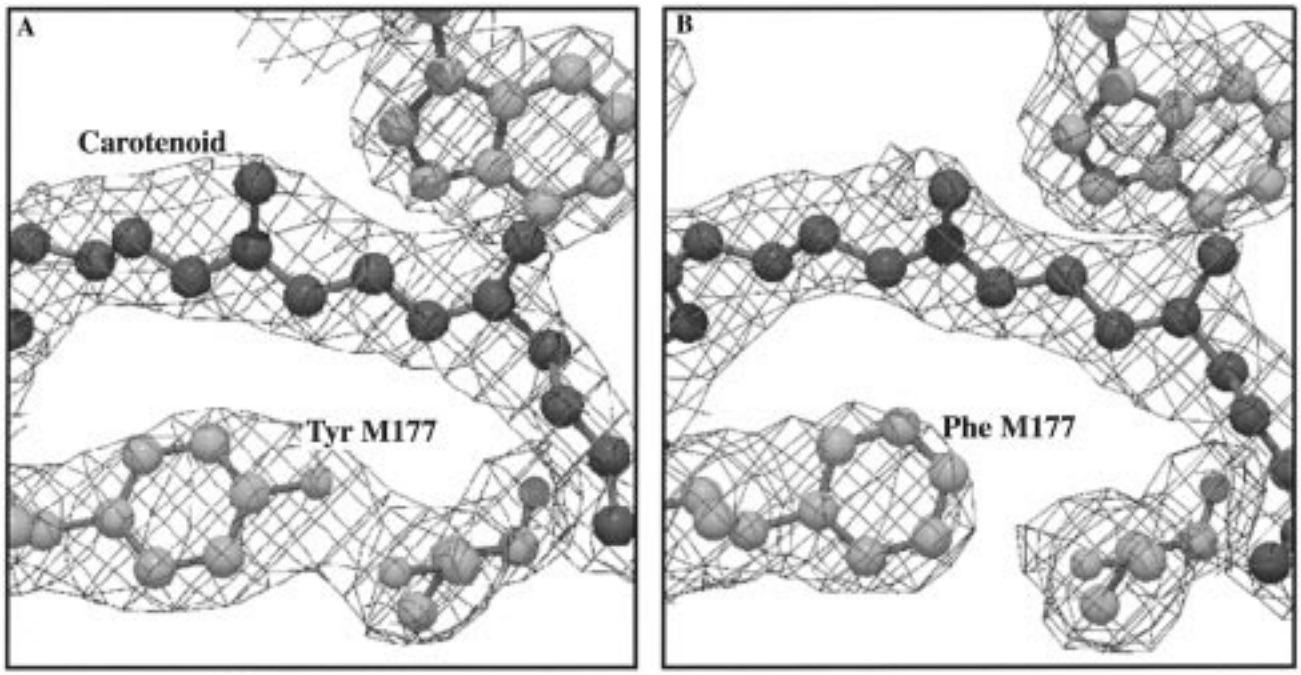

FIGURE 3: Structure of the RC in the vicinity of residue M177 in (A) the WT RC and (B) the FM197R/YM177F mutant RC. Shown are omit $F_O - F_C$ maps contoured at 3.0σ. Residues Trp M157 and Ser M119 are also shown. The figure was prepared using the packages Molscript (*56*), Raster 3D (*57*, *58*), and Minimage (*59*).

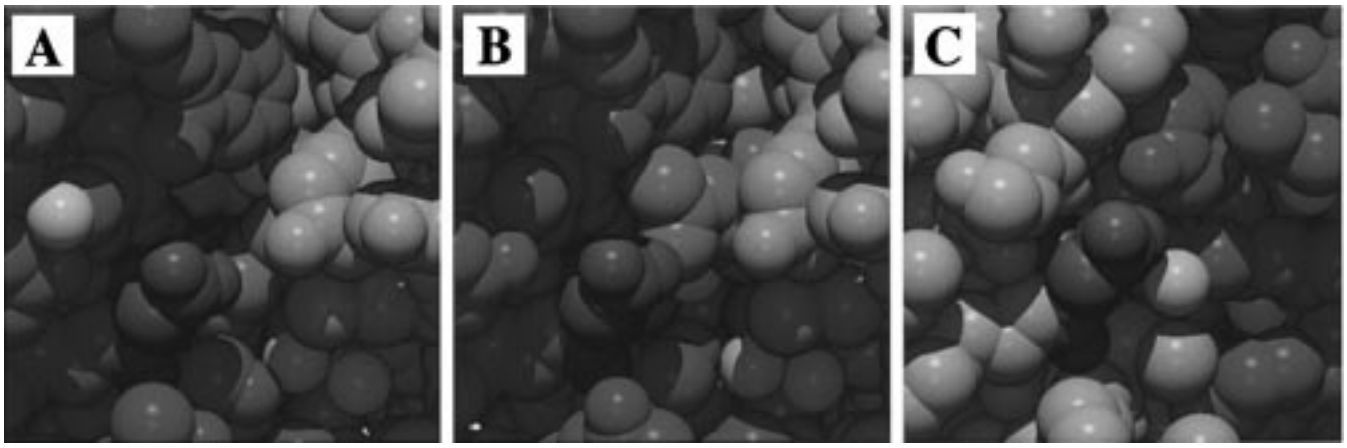

FIGURE 4: View of residues Phe M197 (A), Arg M197 (B), and His L168 (C) from the periplasmic surface of the RC. The M197 and L168 residues are shown in cyan, and Asp L155 (A and B) and Asp M184 (C) are shown in red. For all panels, M subunit residues are shown in yellow and L subunit residues are in green. RC cofactors are in pink, and fixed waters are in white. Panel C has been rotated to give approximately the same view of the M197 and L168 "clefts". The figure was prepared using the packages Molscript (*56*) and Raster 3D (*57*, *58*).

surprisingly, this striking change in orientation did not involve a major rearrangement of the protein. Examination of the structure of the WT protein showed that the aromatic ring of Phe M197 lies at the interface of the M and L subunits and that several of the carbon atoms of the Phe ring are visible from the exterior of the protein due to a cleft that is present between the subunits (Figure 4A). The new Arg residue in the FM197R/YM177F RC was found to lie along this cleft, pointing directly at Asp L155 which had barely changed position relative to the WT structure (Figure 4B compared with Figure 4A). Electron density was seen between the proximal nitrogen of Arg M197 and the proximal oxygen of Asp L155, indicating a salt bridge interaction between the two. These residues were separated by ~2.7 Å, well within the 2.5−4.9 Å range of inter-residue distances cited for possible salt bridge interactions in the RC (*7*). The new orientation for the Arg residue was accommodated by some minor alterations in the position of neighboring residues, particularly Trp L151 and Tyr M198, but there was no significant change in the position of the backbone of either subunit. The shifts observed for Trp L151 and Tyr M198, which are near the surface of the protein, were no greater than those observed for surface residues in other regions of the protein.

The new position for the M197 residue left a cavity in the interior of the protein, adjacent to the P_M Bchl, that was partially filled by a water molecule (Figure 5B). The structural change also involved an alteration in the orientation of the 2-acetyl carbonyl group of P_M, which had undergone a small rotation out of the plane of the P_M macrocycle. It was not possible to distinguish between the oxygen and carbon "arms" of the 2-acetyl group in the electron density map. However, if, as we have indicated in Figure 5, the oxygen of the C═O group points toward the new water

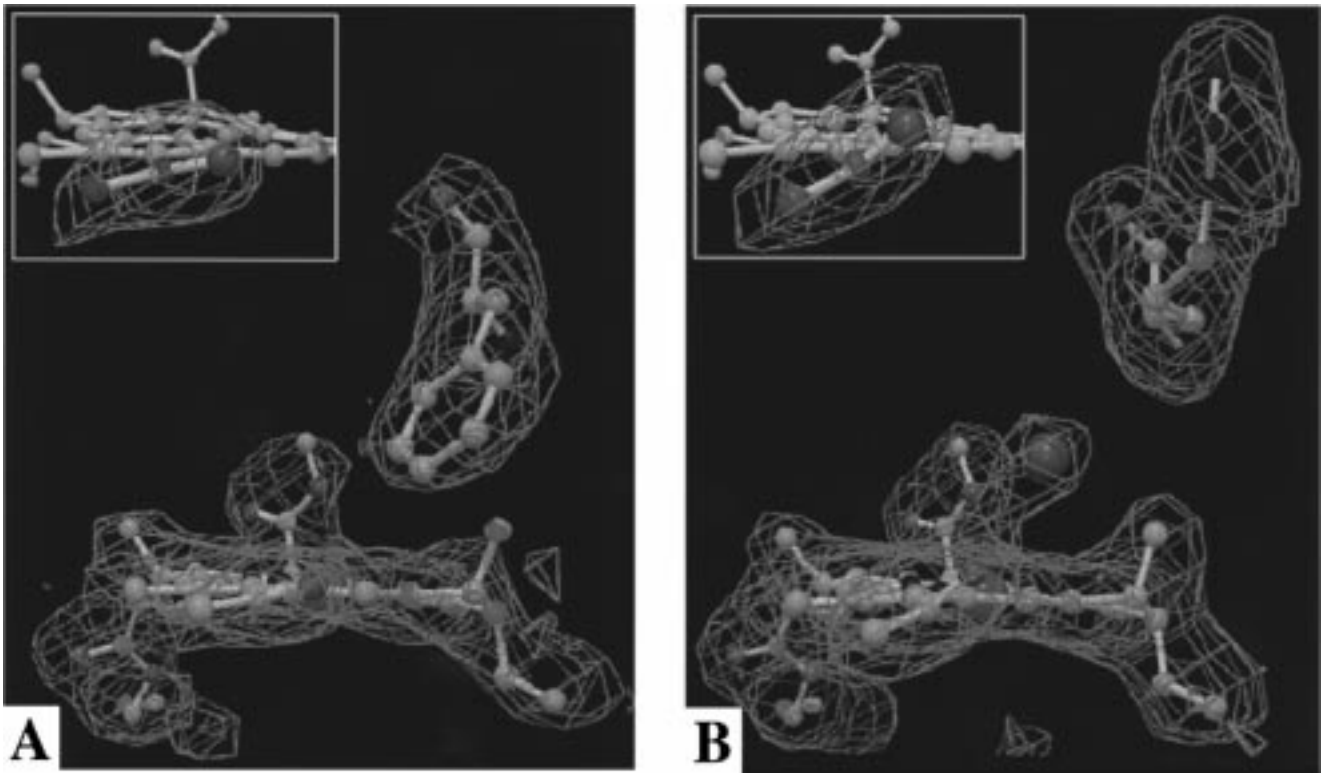

FIGURE 5: Detail of the change in orientation of Arg M197 (B) relative to the position of Phe M197 (A). The carbon atoms of the P_M Bchl and M197 residue are shown in gray, oxygen atoms in red, and nitrogen atoms in blue, and the central magnesium is shown as a light green sphere. In panel B, the new fixed water molecule is shown as a red sphere. The omit $F_O - F_C$ maps are contoured at 3.0σ. Insets in panels A and B show omit $F_O - F_C$ maps contoured at 5.0σ for the 2-acetyl group of P_M, highlighting the rotation of the group relative to the plane of the Bchl ring. The figure was prepared using the packages Molscript (*56*), Raster 3D (*57*, *58*), and Minimage (*59*).

molecule that partially fills the cavity left by the reorientated Arg group, then this would place the oxygen within H bond distance of this new water (2.7 Å). In support of this assignment, it should be remembered that X-ray diffraction is only capable of identifying fixed water molecules, such as those involved in H bond interactions with neighboring groups.

DISCUSSION

Structure of the Rb. sphaeroides RC. Research on the mechanism of light energy transduction has benefited enormously from the availability of high-resolution atomic structures for the bacterial RC. To date, three crystal forms of the *Rb. sphaeroides* RC have been described in detail. The most common is the orthorhombic form, which has given rise to structures at a resolution of 2.8−3.1 Å for the RC from strains R-26, Y, and 2.4.1 (*3*−*7*, *39*−*41*) and at a resolution of 3.0−4.0 Å for seven single-site mutants of the RC from strains 2.4.1 and WS 231 (*11*). A trigonal crystal form has also been reported, giving a structure at 2.65 Å resolution for the RC from strain ATCC 17023 (*24*, *25*). Finally, a tetragonal crystal form has been reported for RCs from a WT strain and strain R-26, which gave data at a resolution of 2.8 Å (*42*). This has recently been improved still further, and two models to 2.2 and 2.6 Å have been published (*43*). Several of these structures have been deposited in the Brookhaven Protein Data Bank.

The crystals generated in this study from antenna-deficient strains of *Rb. sphaeroides* were of the trigonal form and gave structures at 2.6 Å resolution for the WT RC and 2.55 Å resolution for the FM197R/YM177F mutant RC. Detailed descriptions of the structure of the WT *Rb. sphaeroides* RC have been published by several groups (*3*−*7*, *24*, *25*, *39*−*41*) and have shown some variation. The 2.6 Å structure for the WT RC obtained in this study agrees with the assignments for axial ligands to the magnesiums of the RC Bchls (His L153, His L173, His M182, and His M202) and participants in hydrogen bond interactions (such as His L168 and Glu L104) described in refs *24* and *25* (Brookhaven PDB code 1PCR). Conservation between the two structures is very good in the central region of the protein. As with the trigonal crystals used to obtain the 1PCR structure, occupancy of the binding site for the Q_B quinone was rather low in our crystals (∼30%). The Q_B quinone was not removed from the molecular replacement, but simulated annealing omit maps were calculated for this site. The position of the Q_B quinone was essentially the same as that reported by Ermler and co-workers (*24*, *25*).

Effect of the Environment on Structural and Functional Properties of the RC. The question of whether the structure of the RC that is revealed by X-ray crystallography is an entirely accurate and faithful representation of the structure of the RC in the membrane (or even in detergent solution) is an intriguing one. From the data in Figure 1A, for example, it can be seen that that extraction of the RC from the membrane and purification of the complex had a number of small effects on the near-infrared absorption spectrum. Crystallization of the RC complex had little further effect on the spectrum. Similar small shifts were seen in the position of absorbance bands in data from the FM197R/YM177F mutant RC (Figure 2), and in this case, some change in the shape of the P band was also seen on

crystallization of the complex. The conclusion drawn from the spectroscopic data is that, while the overall structural and functional integrity of the RC is preserved on removal of the complex from the membrane, the change of environment is sensed by the RC bacteriochlorin cofactors.

There are a number of additional pieces of evidence that suggest that the properties of the bacteriochlorins and the electron transfer reactions taking place within the RC are sensitive to the environment of the complex. For example, picosecond time scale transient absorption spectroscopy applied to both RC-only membranes and purified RCs has shown that the rate of the first step in transmembrane electron transfer, monitored though decay of the P^* state, is slightly slower in membrane-bound RCs (τ = 4.5 ps) than in solubilized complexes (τ = 3.2 ps) (*20*). We have also established that the midpoint potential of the P/P^+ redox couple is sensitive to the environment of the RC, being between 15 and 40 mV lower when the membrane-bound RC is surrounded by the LH1 antenna complex than in purified RCs or in RCs in antenna-deficient membranes (*20*). Taken together, these studies demonstrate that the structure of the RC, the redox properties of the cofactors, and the rate of processes such as intraprotein electron transfer are sensitive to the environment of the complex but that this influence is relatively small.

Structure of the FM197R/YM177F Mutant RC. The mutation YM177F was made as part of a survey of the influence of polar residues that line the carotenoid binding pocket. The mutation did not appear to bring about any change in the carotenoid content of the RC, or the optical properties of the carotenoid (P. K. Fyfe and R. J. Cogdell, unpublished observations). The mutation also did not bring about any change in the structure of the RC in the vicinity of the carotenoid (Figure 3).

The mutation FM197R was made as part of a survey of residues that are capable of forming a H bond from the M197 position to the 2-acetyl carbonyl of P_M. Previous work by other groups has shown that His and Tyr residues introduced at this position are capable of forming such a bond (*37*, *38*), and in the structure of the *Rps. viridis* RC, a H bond is evident between the equivalent residue Tyr M195 and the 2-acetyl carbonyl of P_M (*1*, *2*). In the case of the FM197R mutation, it was noted that the Q_y band of P was strongly blue-shifted relative to its position in the WT complex. The structural origins of this blue shift are revealed in Figures 4 and 5, and were completely unexpected, with the Arg residue pointing toward the surface of the protein where it probably forms a salt bridge interaction with Asp L155, and the cavity left by this reorientation being partially filled by a water molecule. The optical properties of an FM197K mutant RC were essentially identical to those of the FM197R mutant (data not shown), and it is very likely that a similar reorientation of the M197 residue has taken place in this mutant.

At first glance, it is a little surprising that such a radical change in the position of the M197 residue can occur without causing a significant degree of structural alteration in the surrounding protein. However, examination of the structure of the WT RC reveals a cleft at the interface of the L and M subunits that extends from the surface of the protein down to the Phe M197 residue (Figure 4A). This cleft is lined by residues Asn M195 and Tyr M198 from the M subunit and residues Trp L151, Leu L154, Val L157, and Ser L158 from the L subunit. In the FM197R/YM177F mutant, the M197 Arg lies along this cleft in such a way that the surrounding protein is largely undisturbed. The main effect is an increase in the distance between the M subunit and L subunit residues that line the cleft by an average of 0.5 Å (measured from the α carbons of the residues listed above). On the basis of the errors in the position of α carbons, this was not a significant change in structure. Two water molecules were evident in the WT structure at the surface of the protein just to one side of the cleft leading to the FM197 residue (Figure 4A). These water molecules are also present in the 1PCR structure (*24*, *25*) and were present in our structure for the FM197R/YM177F mutant RC (Figure 4B).

We come now to the question of why the M197 residue undergoes this reorientation following mutation from Phe to Arg. The simplest conclusion is that the new arrangement seen in the FM197R/YM177F mutant structure is energetically more stable than the alternative arrangement where the M197 Arg would be buried in the protein, occupying the volume of the WT Phe residue. Perhaps to be expected is the possibility that it is energetically expensive to bury a highly polar residue within the hydrophobic interior of the protein, although the structure of the WT protein and experiments with mutant complexes have shown that such arrangements do exist or can be engineered. Residues Glu L104, Arg L103, and Arg M132 are found in the vicinity of the Bphes in the WT RC, and are assumed to not to be charged. Furthermore, mutagenesis experiments have shown that acidic and basic residues can be introduced deep within the hydrophobic interior of the protein at position L181 (*44*) and at M203 (*45*). One possibility is that during folding of the protein, perhaps as the L and M subunits come together, the Arg M197 takes up a preferred orientation pointing toward the outer surface of the protein and is able to adopt that conformation in the fully folded complex because the cleft that exists in this region of the protein facilitates this new conformation without disturbing the packing of the surrounding protein. Alternately, it may be that an energetically favorable salt bridge interaction is formed between Arg M197 and Asp L155 as the protein folds and that this arrangement is allowed to persist in the mature complex because of the cleft that accommodates the Arg side chain. One way to test these ideas may be to mutate Asp L155 to a neutral residue, to see whether the reorientation of Arg M197 is dependent on the presence of the Asp residue at the surface of the protein. It will also be interesting to see how the Arg M197 residue will pack in a double mutant in which the cleft was blocked by increasing the volume of the lining residues. Experiments designed to reach this end are currently under way.

Influence of Water Molecules. The reorientation of the Arg residue leaves a cavity in the interior of the protein that is partially filled by a fixed water molecule. This observation is in line with crystallographic studies of other mutant RCs that have shown that a reduction in the side chain volume of a particular residue can lead to the incorporation of one or more water molecules in order to make up the lost volume (K. E. McAuley-Hecht and P. K. Fyfe, unpublished results; see also refs *46* and *47* for related findings in soluble proteins). This observation opens up the more general question of how often newly introduced water molecules play

a part in determining the altered biophysical properties of a mutant RC. The involvement of new water molecules was proposed recently in experiments that showed that the P Bchl dimer was retained in a mutant in which the residue that provides the axial ligand to P_M, His M202, was replaced by Gly (*48*). Previous experiments had shown that replacement of this residue by Leu or Phe resulted in the incorporation of Bphe into the RC at the P_M position, creating a RC with a primary donor consisting of a Bphe−Bchl heterodimer (*49*). In the case of the HM202G mutant, Gly clearly could not provide the axial ligand to Bchl, but it was suggested that the cavity created by the His to Gly mutation was filled by one or more water molecules and that one of these provides the axial ligand to the P_M Bchl (*48*). Our crystallographic data show that this proposal is entirely feasible for a membrane protein, with cavities created in the protein interior by mutagenesis being filled with water molecules.

Orientation of the 2-Acetyl Carbonyl Group of P_M. For the new water molecule we have identified in the FM197R/YM177F mutant RC to show up in the electron density map, it must be fixed in position, suggesting hydrogen bonding to an adjacent group. The new water is within 2.7 Å of one of the arms of the 2-acetyl carbonyl group of P_M, and it is therefore tempting to suggest a H bond interaction between the two. It is not possible to distinguish between the oxygen and carbon arms of the 2-acetyl group from the electron density map, due to their similar size. In the 1PCR structure of Ermler and co-workers, the oxygen is assigned to the arm that points away from Phe M197. However, Ermler et al. (*24*) suggest that the electron density slightly favors the orientation where the oxygen forms the arm that points toward Phe M197, although the opposite assignment is in fact made in the coordinates of the 1PCR structure. In our structure for the WT RC, we have followed the assignment made in ref *24* and positioned the oxygen of the 2-acetyl group of P_M pointing toward the M197 residue. In the FM197R/YM177F mutant, the likelihood of a H bond to the new water molecule has led us to favor the same assignment, as shown in Figure 5. We are currently carrying out spectroscopic experiments to determine whether the 2-acetyl group of P_M is in fact H bonded in the FM197R mutant RC.

As can be seen from Figure 5, the 2-acetyl group of P_M in the WT RC sits slightly out of the plane of the Bchl ring, making an angle of approximately 15°. In the mutant RC, this group has undergone a rotation that places it approximately 35° out-of-plane, representing a 20° anticlockwise rotation compared with that of the WT RC. This change in conformation of the P Bchls perhaps gives some insight into the origin of the 15 nm blue shift of the P Q_y band that is observed in this mutant. The C═O bond of the 2-acetyl group is conjugated to the π-electron system of the Bchl macrocycle, and the orientation of the 2-acetyl group has been calculated to be one of the factors that determines the absorption properties of P (*50*−*52*). In ref *50*, Parson and Warshel calculated that a rotation of the oxygen atom of the carbonyl group of one of the P Bchls from fully in-plane with the macrocycle to fully out-of-plane (i.e., a 90° rotation) should cause an ∼50 nm red shift of the P Q_y band in the *Rps. viridis* RC. This effect arose principally from a decrease in the Q_y transition energy of the individual Bchl (*50*). At first glance, our experimental findings seem to be at odds with this prediction, as the rotation to a more out-of-plane geometry seen in our structural studies is accompanied by a blue shift of the P Q_y band. However, it has to be remembered that the precise position of the oxygen atom is not certain from the electron density, and the environment of the acetyl group changes (i.e., becomes more polar) in the mutant complex. Also, the study by Parson and Warshel predicted that another strong determinant of the energy of the P Q_y transition is the distance between the two halves of the P dimer (in the direction perpendicular to the planes of the Bchl macrocycles). A blue shift of ∼15 nm could thus be accounted for by a decrease in the separation of the two halves of the P dimer of ∼0.1 Å, a structural change which is well below the limits of detection in RC crystallography. On the basis of the present data, we could not detect any significant change in the spacing of the two Bchls of the P dimer.

Our findings are in better agreement with the data of Fajer and co-workers (*51*, *52*), who calculated that an out-of-plane rotation of the 2-acetyl group would cause a spectral blue shift of the Q_y transition, as the carbonyl bond is taken out of conjugation with the π-electron system of the Bchl ring. However, these authors also pointed out the effect on the absorbance properties of P of other factors such as nearby charged amino acids and the inter-Bchl distance. Our conclusion, therefore, is that the rotation of the 2-acetyl group we observe in the FM197R/YM177F mutant, and the accompanying blue shift in the P Q_y absorption band, are in general accord with the prediction that the orientation of the P_M 2-acetyl group will affect the absorbance properties of P. However, we note that there may be other structural changes in the FM197R/YM177F mutant which are below the resolution of the structural data and which would also influence the position of the P Q_y band.

Implications for Possible Structural Changes at His L168. His L168 is the symmetry-related partner to the M197 residue, forming a H bond to the 2-acetyl carbonyl group of P_L. Extensive experiments have shown that replacement of the L168 His residue by Phe results in breakage of this H bond and is accompanied by a blue shift of the P Q_y band of 15 nm (*36*). This blue shift seems to be characteristic of removal of the His residue, as it is also seen to varying amounts (15−25 nm) when the His residue is replaced by Leu, Phe, Lys, Arg, or Glu (J. P. Ridge, D. Spiedel, and M. R. Jones, unpublished observations). In the case of Arg and Lys mutations at the L168 position, the blue shift of the P Q_y band amounts to some 25 nm. The crystallographic results we have described for the FM197R/YM177F mutant open up the possibility that a similar structural rearrangement underlies the absorbance change seen in some or all of the L168 mutants.

The 2-fold symmetry of the RC suggests that a cleft might also be present connecting residue His L168 with the surface of the protein, and indeed, examination of the WT RC structure shows that His L168 is "visible" from the exterior of the protein (Figure 4C). However, comparison with the "M197 cleft" (Figure 4A) shows that the channel to His L168 is considerably more restricted in the WT RC. A number of the residues that line the M197 cleft are conserved at the symmetry-related position, including Asn M195 (as Asn L166), Tyr M198 (as Tyr L169), and Leu L154 (as Leu M183). Two other residues show changes that are reasonably conservative in terms of size, Val L157 (to Thr M186)

and Ser L158 (to Asn M187), while the largest change is Trp L151 (to Phe M180). The surface residue Asp L155 is also conserved at the symmetry-related position (as Asp M184), and two fixed water molecules are also present in this region of the protein. In addition, the backbone atoms of the L and M subunits are closer in proximity to one another in the case of the L168 cleft than in the M197 cleft. For example, measurements with the WT structure show that the distances between the α-carbons of the opposing residue pairs Leu M183−Asn L166 and Phe M180−Tyr L169 in the L168 cleft are 8.9 and 8.4 Å, respectively, while the distances between the analogous pairs Leu L154−Asn M195 and Trp L151−Tyr M198 in the M197 cleft are 11.1 and 9.3 Å, respectively. The net result of these differences in backbone position and residue volume is that the packing of the residues surrounding the L168 cleft is much tighter than is the case for the cleft that accommodates Arg M197 in the mutant structure (Figure 4C compared with Figure 4A), so if a residue were to lie along the L168 cleft, there would probably have to be a more extensive repacking of the neighboring residues than is seen for Arg M197 in the structure of the FM197R/YM177F mutant. Our conclusion from this comparison is that it is not clear whether replacement of the His residue at the L168 position would necessarily be expected to result in reorientation of the residue in some or all of the above mutants, but that in light of the results we have obtained with the FM197R/YM177F mutant RC this is a possibility that should be kept in mind.

Conclusions. To close, the data presented in this report show that it is possible to obtain crystals of WT or mutant RCs from an antenna-deficient strain that diffract to atomic resolution. The structure determined for the WT complex is essentially the same as that determined by Ermler and coworkers for RCs from an antenna-containing strain, using the same crystal form. Data obtained for a FM197R/YM177F mutant RC show an unexpected change in structure, involving the reorientation of the mutated residue, and the incorporation of at least one new water molecule into the structure. We have also observed rotation of the 2-acetyl carbonyl group of one of the primary donor Bchls. The experiments demonstrate the key role that high-resolution structural studies can play in elucidating the details of the molecular basis for altered biophysical properties in mutant RCs. A full biophysical characterization of the FM197R mutant RC, and related mutant complexes, is currently under way.

ACKNOWLEDGMENT

The authors thank Ulrich Ermler, Günter Fritzsch, and Roy Lancaster for their generous assistance in providing their topology and parameter files used in the crystallographic refinement of the models presented and the staff at Daresbury for assistance with the operation of Beamline 9.6.

SUPPORTING INFORMATION AVAILABLE

Comparison of the position of α-carbons in the structures for the WT and FM197R/YM177F RCs determined in this study and the structure for the RC from *Rb. sphaeroides* strain ATCC 17023 determined by Ermler et al. (*24*, *25*) (4 pages). Ordering information is given on any current masthead page.

REFERENCES

1. Deisenhofer, J., Epp, O., Miki, K., Huber, R., and Michel, H. (1985) *Nature 318*, 618−624.
2. Deisenhofer, J., Epp, O., Sinning, I., and Michel, H. (1995) *J. Mol. Biol. 246*, 429−457.
3. Allen, J. P., Feher, G., Yeates, T. O., Rees, D. C., Deisenhofer, J., Michel, H., and Huber, R. (1986) *Proc. Natl. Acad. Sci. U.S.A. 83*, 8589−8593.
4. Allen, J. P., Feher, G., Yeates, T. O., Komiya, H., and Rees, D. C. (1987) *Proc. Natl. Acad. Sci. U.S.A. 84*, 5730−5734.
5. Komiya, H., Yeates, T. O., Rees, D. C., Allen, J. P., and Feher, G. (1988) *Proc. Natl. Acad. Sci. U.S.A. 85*, 9012−9016.
6. Chang, C.-H., Tiede, D., Tang, J., Smith, U., Norris, J., and Schiffer, M. (1986) *FEBS Lett. 205*, 82−86.
7. Chang, C.-H., El-Kabbani, O., Tiede, D., Norris, J., and Schiffer, M. (1991) *Biochemistry 30*, 5352−5360.
8. Parson, W. W. (1991) in *Chlorophylls* (Scheer, H., Ed.) pp 1153−1180, CRC Press, Boca Raton, FL.
9. Fleming, G. R., and van Grondelle, R. (1994) *Phys. Today 47*, 48−55.
10. Arlt, T., Schmidt, S., Kaiser, W., Lauterwasser, C., Meyer, M., Scheer, H., and Zinth, W. (1993) *Proc. Natl. Acad. Sci. U.S.A. 90*, 11757−11761.
11. Coleman, W. J., and Youvan, D. C. (1990) *Annu. Rev. Biophys. Biophys. Chem. 19*, 333−367.
12. Woodbury, N. W., and Allen, J. P. (1995) in *Anoxygenic Photosynthetic Bacteria* (Blankenship, R. E., Madigan, M. T., and Bauer, C. E., Eds.) pp 527−557, Kluwer Academic Publishers, Dordrecht, The Netherlands.
13. Chirino, A. J., Lous, E. J., Huber, M., Allen, J. P., Schenck, C. C., Paddock, L., Feher, G., and Rees, D. C. (1994) *Biochemistry 33*, 4584−4593.
14. Dohse, B., Mathis, P., Wachtveitl, J., Laussermair, E., Iwata, S., Michel, H., and Oesterhelt, D. (1995) *Biochemistry 34*, 11335−11343.
15. Follope, N., Ferrand, M., Breton, J., and Smith, J. C. (1995) *Proteins: Struct., Funct., Genet. 22*, 226−244.
16. Krauss, N., Schubert, W.-D., Klukas, O., Fromme, P., Witt, H. T., and Saenger, W. (1996) *Nat. Struct. Biol. 3*, 965−973.
17. Jones, M. R., Fowler, G. J. S., Gibson, L. C. D., Grief, G. G., Olsen, J. D., Crielaard, W., and Hunter, C. N. (1992) *Mol. Microbiol. 6*, 1173−1184.
18. Jones, M. R., Visschers, R. W., van Grondelle, R., and Hunter, C. N. (1992) *Biochemistry 31*, 4458−4465.
19. Vos, M. H., Jones, M. R., McGlynn, P., Hunter, C. N., Breton, J., and Martin, J.-L. (1994) *Biochim. Biophys. Acta 1186*, 117−122.
20. Beekman, L. M. P., Visschers, R. W., Monshouwer, R., Heer-Dawson, M., Mattioli, T. A., McGlynn, P., Hunter, C. N., Robert, B., van Stokkum, I. H. M., van Grondelle, R., and Jones, M. R. (1995) *Biochemistry 34*, 14712−14721.
21. Beekman, L. M. P., van Stokkum, I. H. M., Monshouwer, R., Rijnders, A. J., McGlynn, P., Visschers, R. W., Jones, M. R., and van Grondelle, R. (1996) *J. Phys. Chem. 100*, 7256−7268.
22. Vos, M. H., Jones, M. R., Breton, J., Lambry, J.-C., and Martin, J.-L. (1996) *Biochemistry 35*, 2687−2692.
23. Buchanan, S. K., Fritzsch, G., Ermler, U., and Michel, H. (1993) *J. Mol. Biol. 230*, 1311−1314.
24. Ermler, U., Fritzsch, G., Buchanan, S. K., and Michel, H. (1994) *Structure 2*, 925−936.
25. Ermler, U., Michel, H., and Schiffer, M. (1994) *J. Bioenerg. Biomembr. 26*, 5−15.
26. Jones, M. R., Heer-Dawson, M., Mattioli, T. A., Hunter, C. N., and Robert, B. (1994) *FEBS Lett. 339*, 18−24.
27. McGlynn, P., Hunter, C. N., and Jones, M. R. (1994) *FEBS Lett. 349*, 349−353.
28. Jolchine, G., and Reiss-Husson, F. (1974) *FEBS Lett. 40*, 5−8.
29. Okumura, M. Y., Steiner, L. A., and Feher, G. (1974) *Biochemistry 13*, 1394−1402.
30. Otwinowski, Z. (1993) in *Data Collection and Processing* (Sawter, L., Isaacs, N., and Bailey, S., Eds.) pp 56−62, SERC Daresbury Laboratory, Warrington, United Kingdom.
31. Navaza, J. (1994) *Acta Crystallogr. A50*, 157−163.

32. Brünger, A. T., Juriyan, J., and Karplus, M. (1987) *Science 235*, 458−460.
33. Jones, T. A., Zou, J. Y., Cowan, S. W., and Kjeldgaard, M. (1991) *Acta Crystallogr. A47*, 110−119.
34. Collaborative Computational Project Number 4 (1994) *Acta Crystallogr. D50*, 760−763.
35. Tiede, D. M., Budil, D. E., Tang, J., El-Kabbani, O., Norris, J. R., Chang, C.-H., and Schiffer, M. (1988) in *The Photosynthetic Bacterial Reaction Center: Structure and Dynamics* (Breton, J., and Verméglio, A., Eds.) pp 13−20, Plenum, New York.
36. Murchison, H. A., Alden, R. G., Allen, J. P., Peloquin, J. M., Taguchi, A. K. W., Woodbury, N. W., and Williams, J. C. (1993) *Biochemistry 32*, 3498−3505.
37. Mattioli, T. A., Williams, J. C., Allen, J. P., and Robert, B. (1994) *Biochemistry 33*, 1636−1643.
38. Wachtveitl, J., Farchaus, J. W., Das, R., Lutz, M., Robert, B., and Mattioli, T. A. (1993) *Biochemistry 32*, 12875−12886.
39. Arnoux, B., Ducruix, A., Reiss-Husson, F., Lutz, M., Norris, J., Schiffer, M., and Chang, C.-H. (1989) *FEBS Lett. 258*, 47−50.
40. El-Kabbani, O., Chang, C.-H., Tiede, D., Norris, J., and Schiffer, M. (1991) *Biochemistry 30*, 5361−5369.
41. Arnoux, B., Gaucher, J. F., and Ducruix, A. (1995) *Acta Crystallogr. D51*, 368−379.
42. Allen, J. P. (1994) *Proteins: Struct., Funct., Genet. 20*, 283−286.
43. Stowell, M. H. B., McPhillips, T. M., Rees, D. C., Soltis, S. M., Abresch, E., and Feher, G. (1997) *Science 276*, 812−816.
44. Schiffer, M., Chan, C.-K., Chang, C.-H., DiMagno, T. J., Fleming, G. R., Nance, S., Norris, J., Snyder, S., Thurnauer, M., Tiede, D. M., and Hanson, D. K. (1992) in *The Photosynthetic Bacterial Reaction Center II* (Breton, J., and Verméglio, A., Eds.) pp 351−361, Plenum Press, New York.
45. Williams, J. C., Alden, R. G., Murchison, H. A., Peloquin, J. M., Woodbury, N. W., and Allen, J. P. (1992) *Biochemistry 31*, 11029−11037.
46. Alber, T., Dao-pin, S., Wilson, K., Wozniak, J. A., Cook, S. P., and Matthews, B. W. (1987) *Nature 330*, 41−46.
47. Buckle, A. M., Cramer, P., and Fersht, A. R. (1996) *Biochemistry 35*, 4298−4305.
48. Goldsmith, J. O., King, B., and Boxer, S. G. (1996) *Biochemistry 35*, 2421−2428.
49. Bylina, E. J., and Youvan, D. C. (1988) *Proc. Natl. Acad. Sci. U.S.A. 85*, 7226−7230.
50. Parson, W. W., and Warshel, A. (1987) *J. Am. Chem. Soc. 109*, 6152−6163.
51. Gudowska-Nowak, E., Newton, M. D., and Fajer, J. (1990) *J. Phys. Chem. 94*, 5795−5801.
52. Thompson, M. A., Zerner, M. C., and Fajer, J. (1991) *J. Phys. Chem. 95*, 5693−5700.
53. Brünger, A. T. (1992) *Nature 335*, 472−475.
54. Laskowski, R. A., MacArthur, W. W., Moss, D. S., and Thornton, J. M. (1993) *J. Appl. Crystallogr. 26*, 283−291.
55. Luzzati, V. (1952) *Acta Crystallogr. 5*, 802−810.
56. Kraulis, P. J. (1991) *J. Appl. Crystallogr. 24*, 946−950.
57. Bacon, D. J., and Anderson, W. F. (1988) *J. Mol. Graphics 6*, 219−220.
58. Merrit, E. A., and Murphy, M. E. P. (1994) *Acta Crystallogr. D50*, 869−873.
59. Arnez, J. G. (1994) *J. Appl. Crystallogr. 27*, 649−653.

BI971717A